THE ASTRONOMICAL JOURNAL VOLUME 106, NUMBER 3 SEPTEMBER 1993

THE DEPENDENCE OF THE COOL MATTER CONTENT ON GALAXY MORPHOLOGY IN GALAXIES OF TYPES E/S0, S0, AND Sa

D. E. HOGG AND M. S. ROBERTS

National Radio Astronomy Observatory,[1] 520 Edgemont Road, Charlottesville, Virginia 22903-2475
Electronic mail: dhogg@nrao.edu, mroberts@nrao.edu

ALLAN SANDAGE

The Observatories of the Carnegie Institution of Washington, 813 Santa Barbara Street, Pasadena, California 91101
Electronic mail: ars@ociw.edu

Received 1993 March 29; revised 1993 May 24

ABSTRACT

Using the material assembled in earlier papers, we examine the manner in which the interstellar matter content varies along the Hubble sequence from S0 galaxies to Sa galaxies selected from the RSA2 compilation. For this we make use of a new and more detailed classification which is described here as applied to these early disk/spiral galaxies. The prominence of the disk in S0's and the visibility of features (H II regions) in the Sa's serve as the basis for the subtypes. Three S0 categories: subtle, intermediate, and pronounced, and four Sa descriptors: very early, early, intermediate, and late are assigned to the galaxies. It is found that the total amount of hydrogen (H I+H_2) is a function of subtype, being low in the S0's and rising smoothly from the early Sa's to the later Sa's. The average surface density of hydrogen exceeds $3\mathcal{M}_\odot$ pc^{-2} only in the latest subtypes of the Sa's. We conclude that the prominence of the disk of a galaxy closely follows the amount of cool gas which the disk contains.

1. INTRODUCTION

The classification S0 was introduced by Hubble as a description of galaxies whose morphological characteristics lie between the disk-dominated spirals and the spheroidal elliptical systems. Since then there has been extensive discussion whether this classification sequence is also an evolutionary sequence. Many studies have focused on a particular feature such as the luminosity profile, the bulge-to-disk ratio or the nature of the interstellar matter, but the question of the evolution remains contentious.

Equally contentious is the question of the classification itself. There usually is no problem for systems with well-developed disks. Many spheroidal systems also are unambiguously classified as ellipticals in most catalogs. There are, however, a number of galaxies for which the classification is badly confused. Some of these are S0's that either have a very subtle disk or whose disk lies within the burn-out image of the bulge, and have therefore been classified as elliptical. Another problem is with Sa galaxies that have arms of low surface brightness, and which therefore have been incorrectly classified as S0's (cf. Eder *et al.* 1991).

The confusion about classification propagates into the discussion of the properties of early-type systems, most notably in the assessment of the gas content measured using the emission lines of H I and CO. Attempts to put the classification system on a quantitative basis, for example, using CCD measures of the brightness profile followed by some type of curve fitting to separate the bulge and disk, have in general been unsuccessful. This failure stems from the unhappy circumstance that the exponential disk profile is very difficult to distinguish from the bulge profile (the $r^{1/4}$ law) in regions where the two overlap.

Despite the difficulty in getting agreement about the classification of any given object, there nevertheless is a smooth progression in the average characteristics of the interstellar medium in going from ellipticals to S0's to Sa's (Bregman *et al.* 1992, Paper II) using the *Revised Shapley–Ames Catalog* (Sandage & Tammann 1981, 1987; hereafter referred to as RSA1 and RSA2) as the source of the classification. But to study this correlation between galaxy morphology and interstellar matter in further detail, we use here a new classification of spiral and disk galaxies. For each class we develop an estimate of the total mass of cool gas and explore the variation of this quantity with galaxy class.

2. THE ADOPTED GALAXY CLASSIFICATIONS

The galaxy types most difficult to classify on low resolution plate material are in the early morphological sections of the classification sequence between the elliptical and the late-Sa types. In the revised and extended Hubble system used in the RSA1 and RSA2 these difficult types are in the E/S0, S0, SB0, S0/a, SB0/SBa, and early parts of the Sa and SBa morphological sections. Examples of the differences in types assigned by different classifiers in these early classification bins can be found by comparing the principal source catalogs such as the *Second and Third Reference Catalogs* of de Vaucouleurs and collaborators (1976, 1991, hereafter referred to as RC2 and RC3), the *Uppsala General Catalog of Galaxies* (Nilson 1973), The *ESO/Uppsala Survey of the ESO (B) Atlas* (Lauberts

[1]Operated by Associated Universities, Inc., under cooperative agreement with the National Science Foundation.

 0004-6256/93/106(3)/907/16/$0.90

1982), and the RSA1 and RSA2. A discussion of the percentage of differences in assigned types as a function of type in these catalogs has been given in Paper II (Bregman *et al.* 1992).

The classification difficulties in this early section of the classification sequence arise from the subtlety of the classification criteria, necessitating high spatial resolution of the galaxy image. The problem is exacerbated by the generally high surface brightness of such galaxies, making classification of them often unreliable using materials with small dynamic range and small plate scale such as paper prints from the Palomar Schmidt Sky Survey. The images are often burned out, eliminating all detail. Indeed, highly inclined galaxies even as late as Sb have been confused with earlier types such as S0 or S0/a in some of the source catalogs just mentioned.

Experience shows that to avoid most of the misclassifications of these early-type galaxies requires about 3000 picture elements in the image. With photographic plates obtained with large plate-scale reflectors such resolutions, at 1 arcsec seeing, can be achieved for all galaxies in the Shapley–Ames Catalog.

The need for adequate classifications is, of course, crucial for the problem being discussed in this series of papers. We are seeking correlations between various physical parameters such as the cold and hot gas content and the galaxy type. Noise in the classification introduces noise in the correlations. Furthermore, conclusions concerning the existence of continuity along the classification sequence are also clouded by inadequate classifications.

The problem is severe, judged by the many recent discussions of the variation of physical parameters along the Hubble sequence (e.g., Knapp *et al.* 1989; Eder *et al.* 1991; Young & Scoville 1991).

We take cognizance of the classification problem here at the outset. Details of the classification of all Shapley–Ames galaxies later than E and earlier than Sab or SBab are set out in this section. The classifications have been made on the large-focal-plane scale telescopes at Mount Wilson, Palomar, and Las Campanas. All plate material have adequate spatial resolution (generally seeing of about 1 arcsec or better with telescopic plate scales of 11 arcsec per mm at Palomar and at Las Campanas, and 16 arcsec per mm at Mount Wilson).

Most of the classifications given in Tables 1–5 here are the same as listed in the RSA2. In addition, subtypes are assigned to the S0 and SB0 types describing the degree of the S0 departure from an E galaxy luminosity profile, as explained below. In addition, the Sa and SBa galaxies are binned into four subtypes describing the position within the Sa and SBa morphological boxes from very early Sa (SBa) to very late. The bulge size and the dust content within the Sa and SBa boxes are also indicated in an extended notation.

A description of the classification criteria, of the extended classification notations, and the tables listing all Shapley–Ames galaxies newly classified in this way are set out in the following subsections. Most of the galaxies listed here are illustrated in the *Carnegie Atlas of Galaxies* (Sandage & Bedke 1993, hereafter referred to as the CAG) where descriptions and explanations are given for the differences in the classifications here from the other current classification catalogs. The illustrations in the CAG are from the same plates used in the new subclassifications detailed here.

2.1 E/S0, S0/E Galaxies

S0 galaxies differ from E galaxies either in the obvious presence of a disk seen in nearly edge on S0 galaxies or by an extended envelope in S0's seen more nearly face on. By definition, neither of these features exist in E galaxies.

E/S0 and S0/E galaxies are neither pure E nor pure S0. The morphology of the central regions are pure E. However, the envelopes in the outer regions are extended, unlike pure E halos. The flattening ratio of the extended envelope is generally different from that of the central E-like bulge, taken to be evidence of a weak disk. Galaxies with the most subtle extended envelopes are E/S0; those where the feature is more pronounced are called S0/E.

The shallow luminosity gradient in the outer envelope is subtle enough that many galaxies now classified as E/S0 or S0/E in the RSA2 are not classified as such in the older literature, based on different plate material. Such differences are often discussed in the descriptions of the photographs in the CAG, to which the reader is referred in individual cases in adjudications of the differences.

Thirty galaxies are listed as E/S0 or S0/E in the RSA2. The table listing them is not repeated here as it is the same as the E/S0, S0/E binning table of the RSA2 (page 73). All galaxies of these types have large bulges and little or no dust. However, the dust content is not a classification criterion. E galaxies exist with dust as well as dust free (to the extent seen by visual inspection of plates). Likewise, S0 galaxies exist that are dust free (the $S0_1$ types) as well as dust rich (the $S0_3$ types described in the next section).

2.2 S0 Galaxies

The S0 classification criteria are twofold. (1) A disk is present, seen either as an extended envelope in nearly face on galaxies, or as a definite disk in nearly edge on galaxies. (2) Spiral structure is totally absent in the disk.

The difference between E galaxies and S0 galaxies resides totally in the presence or absence of a disk. E galaxies, by definition, have no disk; S0 galaxies, by definition, do. The presence or absence of dust plays no role in the classification.

Here we have added a subclassification of "P", "I," or "S" to the formal notation, indicating whether the S0 classification criterion of extended envelope (compared with the sharp cutoff in the luminosity profile of E galaxies) is pronounced, intermediate, or subtle. These subsidiary notations are indicated in the listings in Table 1 (column 3).

In addition, the three types of S0 forms introduced in the Hubble Atlas (Sandage 1961) are retained. In galaxies (each satisfying the three criteria described above) of the $S0_1$ subtype, the luminosity profile is smooth, exhibiting

TABLE 1. Classification of S0 types in RSA.

Name	Type	Subtype	Name	Type	Subtype
N 128	$SO_2(8)$ pec	P	N 4179	$SO_1(9)$	P
N 148	$SO_2(r)(6)$	P	N 4203	$SO_2(1)$	P
N 274	$SO_1(0)$	P	N 4215	$SO_2(9)$	P
N 404	$SO_3(0)$	P	N 4251	$SO_1(8)$	P
N 584	$SO_1(3,5)$	S/I	N 4270	$SO_1(6)$	P
N 890	$SO_1(5)$	I	N 4281	$SO_3(6)$	I
N 1172	$SO_1(0,3)$	S	N 4339	$SO_{1/2}(0)$	S
N 1175	$SO_2(8)$	P	N 4350	$SO_1(8)$	P
N 1201	$SO_1(6)$	P	N 4377	$SO_1(3)$	P!
N 1297	$SO_{2/3}(0)$	I/P	N 4379	$SO_1(2)$	P
N 1332	$SO_1(6)$	P	N 4382	$SO_1(3)$ pec	P
N 1381	$SO_1(9)$	P	N 4386	$SO_1(5)$	P
N 1389	$SO_1(5)/SBO_1$	I	N 4417	$SO_1(7)$	P
N 1411	$SO_2(4)$	P	N 4452	$SO_1(9)$	P
N 1400	$SO_1(1)$	P	N 4460	SO/Sc	-
N 1461	$SO_{1/2}(7)$	P	N 4459	$SO_3(3)$	P
N 1527	$SO_2(6)$	P	N 4474	$SO_1(8)$	P
N 1553	$SO_{1/2}(5)$ pec	P	N 4526	$SO_3(6)$	P
N 1596	$SO_1(7)$	P	N 4552	$SO_1(0)$	S/I
N 1947	$SO_3(0)$ pec	S	N 4578	$SO_{1/2}(4)$	P
N 2310	$SO_{2/3}(8)$	P	N 4638	$SO_1(7)$	P
N 2549	$SO_{1/2}(7)$	P	N 4649	$SO_1(2)$	S
N 2685	$SO_3(7)$ pec	I/P	N 4684	$SO_1(7)$	P
N 2732	$SO_1(8)$	P	N 4696	$SO_3(0)$	I/P
N 2768	$SO_{1/2}(6)$	I	N 4710	$SO_3(9)$	P
N 2784	$SO_1(4)$	P	N 4753	SO pec	S?
N 2902	$SO_1(0)$	P	N 4760	$SO_1(2)$ or cD	I
N 2907	$SO_3(6)$ pec:	P[1]	N 4762	$SO_1(9)$	S
N 2911	$SO_3(2)$ or SOp	S	N 4825	$SO_{1/2}(3)$	I
N 2968	Amorp or SO_3p	-	N 4933	SO_3 pec[2]	P
N 3056	$SO_{1/2}(5)$	P	N 4958	$SO_1(7)$	P
N 3065	$SO_{1/2}(0)$	P	N 4976	$SO_1(4)$	P
N 3098	$SO_1(9)$	P	N 5011	$SO_1(2)$	P
N 3115	$SO_1(7)/a$	P	N 5018	$SO_2(4)/a$	P
N 3203	$SO_2(7)$	P	N 5077	$SO_{1/2}(4)$	S
N 3245	$SO_1(5)$	P	N 5084	$SO_1(8)$	P!
N 3390	$SO_1(8)$ or (Sb)	-	N 5087	$SO_3(5)$	S
N 3607	$SO_3(3)$	S	N 5102	$SO_1(5)$	P
N 3630	$SO_1(9)$	P	N 5128	SO + S pec	S
N 3665	$SO_3(3)$	S	N 5193	$SO_1(0)$	P
N 3957	$SO_3(9)$	P	N 5266	$SO_3(5)$ pec[3]	S
N 3998	$SO_1(3)$	P!	N 5308	$SO_1(8)$	P
N 4008	$SO_1(5)$	I	I 4329	$SO_1(5)$	P
N 4024	$SO_1(2,5)$	P	N 5326	$SO_3(6)/Sa$	S
N 4026	$SO_{1/2}(9)$	P	N 5363	$[SO_3(5)]$	-
N 4033	$SO_1(6)$	P	N 5380	$SO_1(0)$	P
N 4105	$SO_{1/2}(3)$	P	N 5419	$SO_1(2)$	I
N 4111	$SO_1(9)$	P	N 5422	Sa or $SO_3(8)$	P
N 4124	$SO_3(6)$	P	N 5485	$SO_3(2)$ pec[3]	S
N 4128	$SO_1(6)$	P	N 5493	$SO_1(7)$	P

TABLE 1. (continued)

Name	Type	Subtype	Name	Type	Subtype
N 5791	$SO_1(4)$	S	N 7232	$SO_3(7)$ or Sb	S
N 5820	$SO_2(4)$	I	N 7302	$SO_1(4)$	P
N 5838	$SO_2(5)$	P	N 7332	$SO_{2/3}(8)$	P
N 5846	$SO_1(0)$	I	I 5269	$SO_1(7)$/Sa	P
N 5866	$SO_3(8)$	I	N 7457	$SO_1(5)$	I
N 5898	$SO_{2/3}(0)$	I	N 7600	$SO_1(5)$	S
I 4889	$SO_{1/2}(5)$	I	I 5328	$SO_1(3)$	I
N 6861	$SO_3(6)$	S			
N 6893	$SO_3(4)$	P			
N 6958	R?$SO_1(3)$	I/P			
N 7029	$SO_1(5)$	P[4]			
N 7135	SO_1 pec[5]	-			
N 7166	$SO_1(6)$	P			
N 7192	$SO_2(0)$	S			
I 5181	$SO_1(7)$	P			

Notes to TABLE 1

[1] Disk and dust.
[2] (Tides?).
[3] (Prolate).
[4] P, disk.
[5] (Merger).

(by visual inspection of photographic plates) a smooth luminosity profile, albeit with changing gradient, in the image on photographic plates.

Galaxies of the SO_2 subtype show subtle departures from smoothness in the luminosity profile. They are illustrated on panels 38–42 of the CAG. A transition subdivision of $SO_{1/2}$ has also been introduced.

Galaxies of subtype SO_3 (note also the intermediate subdivision $SO_{2/3}$ here) show evidence of dust, either as partial lanes or as complete (circular) dust rings. These rings show no spiral pattern, which, if they had been present would force a classification of early Sa.

Table 1 lists all S0 Shapley–Ames galaxies from the binning table of RSA2 (pages 73–75). The new notations of P, I, or S are listed in column 3.

2.3 SB0 Galaxies

The three subtypes of SB0 galaxies introduced in the Hubble Atlas (Sandage 1961) are defined by the character of the bar. (Note the difference in the meaning of the notation for the S0 subtype symbols compared with the same symbols here for SB0 galaxies. The symbols for the S0 galaxies refer to the dust content; the symbols here for SB0's refer to the nature of the bar.)

The "bar" in $SB0_1$ galaxies is a simple deviation from elliptical symmetry where the central bulge is an oval whose major axis is at an angle with the major axis of the intermediate disk and the external envelope. The bar in $SB0_2$ galaxies extends only partway across the intermediate disk. It is indistinct in the inner regions of the image; it continues, after a gap, onto an external ring (or partial rim), forming two opposite regions of enhanced luminosity. The bar is defined by the two bright ansae on the rim of the intermediate luminosity zone. These ansae are at diametrically opposite sides of the lens (or inner disk). The appearance is that of an incomplete bar.

Galaxies with a well-defined sharp bar across the entire disk are called $SB0_3$.

The envelope extents, typed as either P, I, or S, in the same sense as for the S0 galaxies described above, are listed in Table 2. In those SB0 galaxies where the "bar" are the ansae on the rim of a ring surrounding the inner lens, it is not always appropriate to define the extent of the envelope extension (the P, I, S notation) because the structure ends on the ring; there is no extended envelope. For such galaxies, column 3 of Table 2 is usually blank.

The SB0 class is here defined by the absence of arms, and the presence of a bar. Invariably, in such galaxies no recent star formation is evident. From this it is inferred

TABLE 2. Classification of SB0 types in RSA.

Name	Type	Subtype	Name	Type	Subtype
N 16	$SBO_1(4)$	S	N 4346	$SBO_1(8)$	P
N 1023	$SBO_1(5)$	P	N 4371	$SBO_{2/3}(r)(3)$	-
N 1387	SBO_2 (pec)	I/P	N 4425	SB0p or Sap	I
N 1389	$SO_1(5)/SBO_1$	I	N 4435	$SBO_1(7)$	P
I 2035	$SBO_1(4)$ pec	I	N 4442	$SBO_1(6)$	P
N 1574	$SBO_2(3)$	P	N 4483	$SBO_1(5)$	-
N 2646	SBO_2	-	N 4612	$RSBO_{1/2}$	P
N 2859	$RSBO_2(3)$	-	N 4754	$SBO_1(5)$	P
N 2880	SBO_1	I	N 5195	SBO_1 pec	-
N 2950	$RSBO_{2/3}$	-	N 5365	$RSBO_{1/3}$	-
N 3384	$SBO_1(5)$	P	N 5473	$SBO_1(3)$	P
N 3412	$SBO_{1/2}(5)$	P!	N 7155	SBO	-
N 3458	SBO_1	P!	N 7744	$SBO_1(3)$	P
N 3516	$RSBO_2$	I			
N 3892	SBO_2	-			
N 3945	$RSBO_2$	-			
N 4233	$SBO_1(6)$	P			
N 4262	SBO	P			
N 4267	SBO_1	P			
N 4340	$RSBO_2$	-			

that star formation rate in all SB0 galaxies is as small as in the E/S0 and the S0 types.

2.4 S0/a, S0/Sa, SB0/a, and SB0/SBa Galaxies

Thirty-nine galaxies of these intermediate types are listed in Table 3.

The discriminating criterion for the various galaxies of these types is a departure of the luminosity profile from the strict elliptical symmetry that characterizes the smooth S0 types. The departure is caused by two diametrically opposite luminous features emerging from the bulge. These features are not parts of *circular* arcs such as in the shells around some E galaxies, but rather they spiral outward like the more conspicuous real *arms* in the earliest part of the Sa and SBa sequence. They are spiral *sweeps* in the underlying disk rather than well defined relatively thin arms. The features are massive in the sense of Reynolds (1927a,b) and are sometimes described as embryonic arms.

The features are very subtle. They are almost always missed on small-scale plates. Galaxies of this type are not well represented in some of the classification catalogs mentioned earlier.

Beginning with these types, as listed in Table 3, we have added three subsidiary descriptions of arm, bulge, and dust content. The arm types, to be continued into the Sa and SBa lists of Tables 4 and 5, are in four bins as VE, E, I, and L, describing the lack (or otherwise) of the resolution of the "arms" into knots and stars. In an obvious notation, the symbols mean "very early," "early," "intermediate," and "late." The bulge notations of L, I, and S mean "large," "intermediate," and "small." The dust content ranges from 0 to 1; zero meaning no detectable dust upon inspection of the image on the existing photographic plates.

2.5 Sa Galaxies

Sa galaxies are the earliest of the spirals having well defined arms. True arms, in contrast to the embryonic arms of the S0/Sa types, first appear in this section of the classification sequence.

The threefold classification criteria for Sa galaxies are (1) the bulges are generally large, (2) the arms are tightly wound as defined by the small opening angle of a fitted logarithmic spiral (Kennicutt 1981), and (3) the rate of recent star formation, judged by the frequency of bright stars and H II regions, is near zero in the arms of the earliest Sa types (the very early smooth-armed Sa galaxies), and is small but finite in the later part of the Sa morphological box.

Because the length of the Sa section along the classification sequence is so large, the Sa box, as in the S0/Sa types described above, has been divided into the same four sub-boxes of VE, E, I, and L defined by the resolution of the arms into stars and H II regions. As before, the bulge size and the dust content are also noted. These subtypes are indicated in Table 4 by the same symbols as in the S0/Sa section described earlier.

The VE arm types, whose prototypes include NGC 2855, NGC 3271, NGC 3281, NGC 3301, NGC 4461, and NGC 6340 (photographs and descriptions are in the

TABLE 3. Subclassification of RSA S0/Sa and SB0/SBa types.

Name	Type	Sub-Type	Bulge[1]	Dust[2]	Name	Type	Sub-Type	Bulge[1]	Dust[2]
N 254	$RSO_1(6)/Sa$	VE	L	0	N 4477	$SBO_{1/2}/SBa$	VE	L	0
N 474	RSO/a	VE	L	0	N 4546	SBO_1/Sa	VE	I	0
N 524	SO_2/Sa	VE	I	0	N 4608	SBO_3/a	E	L	0
N 936	$SBO_{2/3}/SBa$	VE	L	0	N 4643	SBO_3/SBa	E	L	0
N 1380	$SO_3(7)/Sa$	VE	L	0	N 4665	$SBO_{1/3}/SBa$:	E	L	0
N 1440	$SBO_{1/2}/a$	VE	I	0	N 4767	SO/a	VE	L	0
N 1533	$SBO_2(2)/SBa$	VE	L	0	N 4856	$SO_1(6)/Sa$	E	L/I	0
N 1543	$RSBO_{2/3}(0)/a$	VE	L	0	N 5018	$SO_2(4)/a$	VE	L	1/4
N 2787	SBO/a	VE	L	0	N 5273	SO/a	VE	L	0
N 2962	$RSBO_2/Sa$	VE	I	0	N 5326	$SO_3(6)/Sa$	E	I	1/2
N 3300	SBO_3/a	VE	L	0	N 5574	$SO_1(8)/a$	VE	L	0
N 3414	$SO_{1/2}(0)/a$	VE	L	0	N 5631	$SO_3(2)/Sa$	VE	L	1/4
N 3489	SO_3/Sa	E	I	3/4	N 6875	SO/a (merger)	VE	L	0
N 3637	$RSBO_{2/3}/SBa$	VE	L	0	I 5063	$SO_3(3)$ pec/Sa	I	L	3/4
N 3941	$SBO_{1/2}/a$	VE	L	0	N 7007	$SO_{2/3}/a$	VE	L	1/4
N 4036	$SO_3(8)/Sa$	VE	L	1/4	N 7020	$RSO_2(5)/RSa$	E	I	0
N 4106	SBO/a (tides)	VE	L	0	N 7049	$SO_3(4)/a$	E	L	1/4
N 4143	$SO_1(5)/Sa$	VE	L	0	N 7377	$SO_{2/3}/Sa$ pec	E	L	1
N 4150	$SO_3(4)/Sa$	VE	I	0	N 7585	$SO_1(3)/Sa$	VE	L	0
N 4429	$SO_3(6)/Sa$ pec	VE	I	0					

Notes to TABLE 3

[1] Prominence of bulge. L = large, I = intermediate, S = small.
[2] Visual appearance of dust content. 0, none; 1, large.

CAG) are the smooth-armed Sa galaxies with spiral arms but with no evident recent star formation nor high dust content (e.g., see Kennicutt & Edgar 1986). Evidence suggests that such types are generic to the classification sequence rather than being the result of environmental processes such as stripping (Sandage 1983).

2.6 SBa Galaxies

SBa galaxies are similar to their Sa counterparts in the subtypes of arm types (VE, E, I, and L), in the bulge size (L, I, and S), and in their dust content (0 to 1). These subtypes are indicated in columns 3–5 of Table 5 containing the same galaxies as in the RSA2 binning table (RSA2, page 77).

The very early (VE) SBa prototype of smooth-armed barred spiral is NGC 7743 as discussed by Kennicutt & Edgar (1986). Again, it was the existence of this galaxy and others like it in the isolated field that provided the principal evidence that smooth-armed Sa and SBa galaxies are generic to the classification sequence, not a result of environmental processes (Sandage 1983). This can be used as evidence that initial conditions (such as the strength of the density contrast $\delta\rho/\rho$ of the protogalaxy) rather than subsequent evolutionary processes determine the present Hubble type for most galaxies (Roberts 1963; Sandage *et al.* 1970).

3. THE COLD INTERSTELLAR MEDIUM IN THE GALAXIES

3.1 The Statistics of the Detections

It was noted in Paper I (Roberts *et al.* 1991) that the rates at which the various tracers of the interstellar medium (ISM) in early galaxies were detected are a strong function of the galaxy type, using the classification from the RSA2 catalog. We plot in Fig. 1 the rates with which neutral hydrogen and infrared emission are detected as a function of the galaxy types and subtypes used here. The figure shows the expected trend of higher detection rates in the later galaxy types, but it also shows that the subdivisions of the S0 and Sa classes described in Sec. 2 appear to fit naturally into a sequence of increasing amounts of cold interstellar material. The most dramatic change is with the neutral hydrogen. It is much easier to find hydrogen in S0 (P) than in S0 (S), and it much easier to find in Sa (L) than in Sa (VE). The *IRAS* detections show a similar though less pronounced effect. This is important because

TABLE 4. Subclassification of RSA Sa galaxies.

Name	Type	Sub-Type	Bulge[1]	Dust[2]	Name	Type	Sub-Type	Bulge[1]	Dust[2]
N 718	SaI	E	L	0	N 4224	Sa	E	S/I	1
N 788	Sa	E	L	0	N 4235	Sa	E	I/S	1/2
N 1079	Sa(s)	E	I/L	0	N 4274	Sa(s)	I	I/L	1
N 1302	Sa	E	L	0	N 4293	Sa	I	S	1
N 1316	Sa pec	VE	L	1/4	N 4324	Sa(ring)	I	I	1/2
N 1317	Sa	E	I	1/8	N 4378	Sa(s)	I	I	0
N 1350	Sa(r)	L	I	1/2	N 4419	Sa[2]	-	-	-
N 1357	Sa(s)	I	I	1	N 4424	S(a?) pec	I	I	1/2
N 1371	Sa(s)	E/I[1]	I	1/4	N 4425	SBOp or Sap	VE	S/I	0
N 1386	Sa	E/I	I	1	N 4448	Sa (late)	L	L	1
N 1415	Sa/SBa late	I	I	1	N 4454	Sa	I	I	1/4
N 1617	Sa(s)	I	L	1	N 4461	Sa	VE	L	0
N 1638	Sa	E	L	1/4	N 4503	Sa	VE	L	0
N 2179	Sa	E	I/L	1/4	N 4580	Sc(s)/Sa	-	-	-
N 2639	Sa	I	L	1/2	N 4586	Sa	E/I	S	1
N 2655	Sa pec	E	L	1	N 4698	Sa	E/I	I	1/2
N 2681	Sa	E	L	1/4	N 4699	Sab(Sr)[3]	I	L	1/3
N 2775	Sa(r)	I	L	1/3	N 4772	Sa:	I	I/L	1
N 2781	Sa(r)	I	L	1/3	N 4845	Sa	I	S	1
N 2782	Sa(s) pec	E/I	I	1	N 4866	Sa	E/I	I/S	1/3
N 2811	Sa	E	I	1/2	N 4984	Sa(s)	E	L	1
N 2844	Sa(r)	I:	S:	1:	N 5064	Sa	L	L	1
N 2855	Sa(r)	VE	L	1	N 5121	Sa	VE	L	0
N 2992	Sa (tides)	E	L	1	N 5377	SBa or Sa	I	I	1/2
N 3032	RSa pec	VE	I	1/4	N 5422	Sa or SO_3(8)	E	S	0
N 3166	Sa(s)	I	L	1	N 5448	Sa(s)	L	S	1
N 3190	Sa	E/I	L	1	N 5548	Sa	E/I	I	1/2
N 3271	Sa	VE	I/L	0	N 5614	Sa(s) (tides)	E/I	I	1
N 3277	Sa(r)	I	I/S	1/2	N 5665	Sa/Sc	-	-	-
N 3281	Sa	VE	S	1/2	N 5689	Sa	E	L	1/3
N 3301	Sa	VE	S	0	N 5739	Sa(s)	E	I	1/3
N 3358	Sa(r)I	I	I	1/2	N 5854	Sa	E	S/I	0
N 3449	Sa	I	I/L	1/2	N 6340	Sa(r)I	VE	L	1/4
N 3571	Sa	I	I/S	1	New 5	Sa(s)	E	I/S	0
N 3593	Sa pec	I	I	1	N 6902	Sa(r)	I/L	S	1/2
N 3611	Sa	I	I	1/3	N 6935	Sa(r)	L	S/I	1
N 3619	Sa	I	L	1	N 7096	Sa(r)I	I	L	0
N 3623	Sa(s)	L	S	1	I 5135	Sa pec	E/I	L	1/2
N 3626	Sa	E	I	1/2	N 7213	Sa(rs)	I	L	3/4
N 3885	Sa	E	S	1	I 5267	Sa(r)	I/L	L	1
N 3898	SaI	I	L	1	N 7679	Sc(s)/Sa[4]	?	L	1
N 3900	Sa(r)	I/L	I	1	N 7702	RSa(r)	[5]	-	1/3
N 4138	Sa(r) pec	I	S	1/2	N 7727	Sa pec	VE	L	1/2
N 4158	Sa:	I:	I:	1:	N 7742	Sa(r!)	[5]	-	1/2
N 4220	Sa(r)	I	S	1					

Notes to TABLE 4

[1] Outer arms are late, inner are E/I.
[2] (Dust only).
[3] Or Sa.
[4] (Tides?).
[5] Ring.

the observations of the sample are more complete in the infrared, whereas the hydrogen studies are very incomplete and extremely heterogeneous.

The use of detection rates is obviously the simplest of tests and may actually reflect a trend of some other parameter of the galaxies in the RSA, e.g., distance or absolute magnitude with subtype. We will explore such possibilities in the following sections by considering the amount of cool gas rather than merely its presence. Anticipating the result of these analyses, we will find that both the absolute amount of interstellar material and the normalized, distance-independent mass-to-luminosity ratio show trends similar to those in Fig. 1. More pronounced disks are in an environment of more interstellar matter.

3.2 The Masses of the Cold Components

We begin by comparing the masses of the ISM components as tabulated in Paper I with the galaxy types as categorized under the classifications used here. We will henceforth no longer consider ellipticals, because there are too few of them in our sample that have been detected in H I or CO. The masses of the atomic hydrogen component are obtained directly from the observed H I flux in the cases of detection, and with only an assumption about linewidth in the cases of upper limits. The mass of molecular material is derived from the CO flux, with assumptions about the distribution of the molecular material and using the galactic conversion factor to relate CO to molecular hydrogen. The dust mass is inferred from the 60 and 100 μm *IRAS* fluxes using the standard model of grain emissitivity and a color temperature based on the 60/100 flux ratio. In calculating the masses, distances based on a Hubble constant of 50 km s^{-1} Mpc^{-1} were used.

The distribution of the masses of the three cold components as a function of galaxy type are given in Figs. 2(a)–2(c). In general the later galaxies have a significantly greater mass of cold gas than do the earlier types. There are only a few S0(S) galaxies with H I content greater than $10^9 \mathcal{M}_\odot$, but there are also a number of very early galaxies for which the *upper limit* for H I is $10^{7.5} \mathcal{M}_\odot$. The masses in the H I and H_2 components are generally comparable, although there are individual objects in which one of the two is dominant. The dust mass is, as expected, much lower than the gas mass, by a factor of roughly 500–1000, in agreement with earlier studies such as Thronson *et al.* (1989).

To facilitate the comparison of the three components, we will use survival analysis techniques (Feigelson & Nelson 1985; Isobe *et al.* 1986) as implemented in the program ASURV (LaValley *et al.* 1992). The data are a mixture of detections and upper limits and are therefore not amenable to analysis by the usual statistics. To take full advantage of the information contained in the distribution of the upper limit values (the "censored" data), we will use the Kaplan–Meier estimator to evaluate the mean value of the sample at each galaxy type for each tracer. This is a unique, self-consistent, maximum-likelihood estimator for the population from which the randomly censored sample has been drawn. It uses both the detections and the upper limits in making the estimate of the median and mean of the sample. The means and their estimated uncertainties are shown in Fig. 3(a).

The mean values of the masses of each component increase smoothly from the later S0 subtypes to the later-Sa subtypes. The data are poorly sampled in the earliest types, with most observations contributing only upper limits, and so the details of the distribution of mass for these classes are not established. The S0 (S) subtypes perhaps have more cool material than the later S0's, though still less than the earlier Sa's.

We now examine the question of the possible biases in the data, and explore whether such biases might produce the effect shown in Fig. 3(a). Because the samples in all wavelengths are flux limited, the amount of cool material found could arise because of large differences in the mean distance of one subclass compared to another. To demonstrate that the mean volumes sampled for the S0's and the Sa's are comparable, the mean blue luminosities of each type have been calculated and summarized in Table 6. The range in luminosities within a type is large, typically a factor of six, whereas the range in the mean is less than a factor of three, and with the exception of the S0(P) and S0/Sa subtypes the means lie within a range of a factor of 2. In addition, the mean distances and the ranges in the distances are similar for all groups, although the spread is so large that this agreement lends only weak support. We conclude that the biases that are distant dependent are likely to be similar from one group to the other, and that the trends demonstrated in Fig. 3(a) reflect the intrinsic properties of the galaxies.

We have also considered other selection effects that might be responsible for the correlation between mass of cold matter and galaxy subtype. The following quantities were examined and show no trend with subtype: apparent magnitude, angular diameter, inclination, and blue luminosity. We conclude that the results here do not arise because of bias in these parameters.

We have examined the H I detection statistics for a subsample of galaxies which lie outside the boundaries of the two principal clusters represented in the RSA, Virgo, and Fornax. The results are similar to that found for the entire sample. Averages of several subtypes (to improve the statistics) show that they are, to within a factor of 2, equally represented in (and out of) clusters.

As a final check, the masses of the cool components in each galaxy have been normalized to the blue luminosity of the galaxy, and the means of the normalized quantities have been calculated as in the manner described for the data of Fig. 3(a). The results are shown in Fig. 3(b). The trend is similar to that found in Fig. 3(a). The scatter of the individual values about the mean is slightly reduced, but is still a factor of four or five, implying that the intrinsic amount of cool matter that may be found in a given galaxy can vary over a wide range.

TABLE 5. Subclassification of RSA SBa galaxies.

Name	Type	Sub-Type	Bulge[1]	Dust[2]	Name	Type	Sub-Type	Bulge[1]	Dust[2]
N 357	SBa	VE	I/L	0	N 5377	SBa or Sa	I	I	1/2
N 1022	SBa(r) pec	E	I/S	1	N 5566	SBa(r)II	I	L	1/2
N 1169	SBa(r)I	I	I/L	1	N 5701	(PR)SBa	E	L	0
N 1291	SBa	VE	L	1/8	N 5750	SBa(s)	I	I	1/2
N 1326	RSBa	E	L/I	1/8	N 5864	SBa	E	I	0
N 1358	SBa(s)I	I	I	1/2	N 6684	SBa(s)	E	L	0
N 1415	Sa/SBa (late)	I/L	S/I	1	N 6942	SBa(s)	E	I	0
N 1452	SBa(r)	E	I	0	N 7079	SBa	VE	L/I	0
N 2217	SBa(s)	I	I	0	I 5240	SBa(r)	L	L	1/2
N 2798	SBa(s) tides	I	I	1	N 7371	SBa(r)II	L	L	1/2
N 2983	SBa	VE	L	0	N 7410	SBa	I/L	L	1
N 3081	SBa(s)	[1]	-	1/3	N 7743	SBa	VE	L	0
N 3185	SBa(s)	[1]	-	1/2					
N 3783	SBa(r)I	I	I	1/4					
N 4245	SBa(s)	I	I	1/3					
N 4260	SBa(s)	E	I	1/4					
N 4314	SBa(rs) pec	E	L	0					
N 4596	SBa[2]	VE	L	0					
N 4795	SBa(s)[3]	E	L	0					
N 5101	SBa	E	L	0					

Notes to TABLE 5

[1] Ring.
[2] (Very early).
[3] (Tides?).

3.3 The Total Mass of Cold Matter in Galaxies

Each of the tracers represents an incomplete description of the total interstellar matter content of a galaxy. For example, galaxies which lie near the center of rich clusters may have relatively less atomic hydrogen, for reasons that are still uncertain but which might be related to the passage of the galaxies through a dense intracluster medium (cf. Haynes *et al.* 1984). It has also been suggested that the relative amount of atomic and molecular gas is a function of the morphological type of the galaxy (Young & Scoville 1991), although the evidence is still being reviewed. It is clear, therefore, that the best measure of the total cool gas component is a combination of the individual estimates.

The simplest of the quantities to derive is the amount of atomic hydrogen. If the galaxy has been detected in the 21 cm line, the conversion of the observed flux to total neutral hydrogen mass is straightforward (cf. Roberts 1975), with the principal uncertainty arising from the uncertainty in the distance to the galaxy. If only an upper limit is measured, than an additional error may be introduced by the assumption concerning the possible velocity width over which the profile should be analyzed.

The CO measurements suffer from three serious limitations. First, the factor with which the CO flux is converted into mass of molecular hydrogen is drawn from studies of molecular clouds in our Galaxy. Estimates for galaxies are generally consistent with the Galactic value (cf. Knapp *et al.* 1987) but there is evidence that the ratio could be a function of metallicity (Maloney & Black 1988). Next, the CO may be poorly sampled, since the beam sizes used in typical galaxy studies are small in comparison with the size of the galaxies and the CO could well lie outside the region studied, especially if the molecular gas occurs primarily in a ring a few kiloparsec from the center of the galaxy. Finally, and of most importance, there are simply too few studies of CO in these galaxies to permit a definitive statistical analysis.

The best sample is of the infrared emission, due, in large measure, to the extensive survey by Knapp *et al.* (1989). Unfortunately it is difficult to convert the infrared fluxes into dust mass because the conversion depends sensitively on the radiative properties of the dust grains and on the grain temperature. However, the dust itself contributes less than one percent of the total mass in the cold component

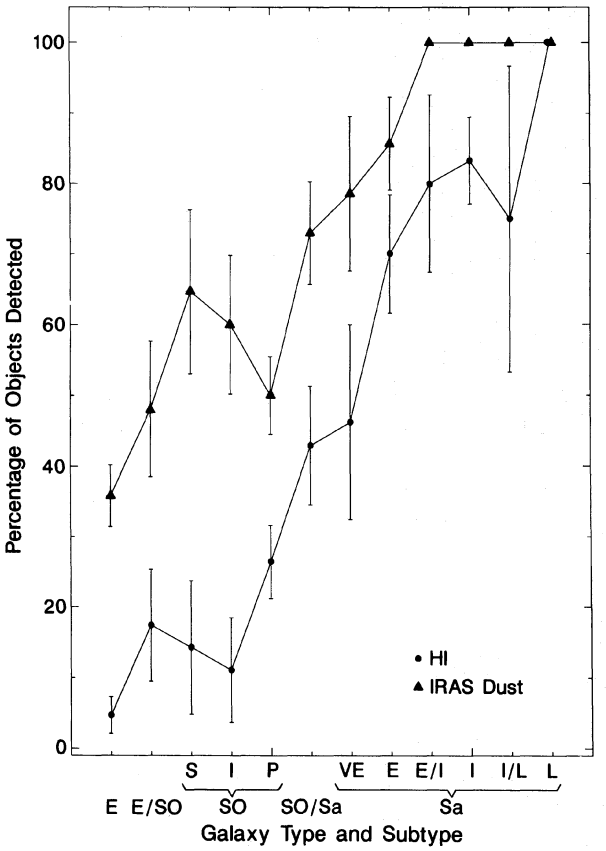

FIG. 1. The rates with which neutral hydrogen and infrared emission are detected, as a function of galaxy subtype. The galaxy types as assigned in the RSA2 range from E to Sa. The galaxy subtypes for S0 and Sa galaxies are described in the text. The uncertainties are based simply on the counting statistics.

and so the uncertainties are unimportant. But because of the poor sampling in H I and especially in CO, the *IRAS* flux is sometimes used as an estimator of gas mass, in which case the uncertainty in the conversion factor is greatly compounded by the additional uncertainty in the gas-to-dust ratio.

We therefore assign the highest weight to the H I data in developing our estimate of the total mass of cool interstellar matter. If there is a detection of H I, we get the total mass by adding to the neutral hydrogen mass the molecular gas mass derived either from a detection of CO, or by a conversion of the *IRAS* flux. The latter quantity is obtained from the relationship found for the objects in this study that are detected in both the infrared and CO [see Paper II, Eqs. (1) and (2)]:

$$\mathrm{Log}\,\mathcal{M}(\mathrm{H_2}) = 4.04 + 2\times\mathrm{Log}(D) + \mathrm{Log}(\mathrm{Sco})\,, \qquad (1)$$

$$\mathrm{Log}(\mathrm{Sco}) = -1.76 + \mathrm{Log}(\mathrm{S100}). \qquad (2)$$

Here Sco is the inferred CO flux in Jy km/s, S100 is the measured flux density at a wavelength of 100 μm in mJy, D is the distance in Mpc, and $\mathcal{M}(\mathrm{H_2})$ is the inferred mass of molecular material, in solar units.

If the object is detected in the infrared but not in H I, the mass of the cold gas component might in principle be estimated from the infrared emission. We begin by plotting in Fig. 4 the mass of the neutral hydrogen as a function of the mass of dust inferred from the *IRAS* flux. The scatter is large, as has been noted in earlier studies (cf. Young *et al.* 1989; Eskridge & Pogge 1991). The dashed line is the line of best fit with slope of unity, a value suggested earlier by Young *et al.* who included galaxies of later types. The least-squares fit to the data from our survey for galaxies in which both H I and *IRAS* have been detected is given by the solid line. The fit is made in the sense of H I upon *IRAS*, since the sole purpose of this analysis is to provide a means by which the *IRAS* data may be used to estimate hydrogen mass. The values for the dwarf systems NGC 185 and NGC 205 have been omitted from the analysis, since they significantly affect the regression parameters and yet lie well outside the mass ranges of interest. We will use the relationship shown by the solid line:

$$\mathrm{Log}(\text{Mass of HI}) = 6.10 + 0.52\times\mathrm{Log}(\text{Mass of Dust}). \qquad (3)$$

The total gas mass as estimated from the infrared measurement alone is derived from Eq. (3) by adding an estimate of the molecular component to give

$$\mathrm{Log}(\text{Total Gas Mass}) = 6.25 + 0.52\times\mathrm{Log}(\text{Mass of Dust}). \qquad (4)$$

For those galaxies not detected in any tracer, the upper limit to the cold matter is taken to be twice the H I limit, or, if that was not available, twice the infrared limit.

Figure 5 shows the estimated total mass of interstellar hydrogen, both atomic and molecular, as a function of galaxy subtype. The mass for each galaxy has been normalized by the object's total blue luminosity. The points shown are the estimated means and errors in the means as derived using both detections and upper limits. As was the case for the individual tracers, there is a pronounced trend for the total mass of interstellar matter to increase from the early S0's through the latest Sa's. Two-sample tests utilizing the censored data show that the likelihood of the S0(S) and the Sa(L) groups being drawn from the same parent population is less than 0.1 percent. The difference between the S0(P) and the Sa(L) is similarly marked. In contrast the early Sa's are statistically much like the S0's. For example, there is a 50 percent chance that the Sa(VE) galaxies are drawn from the same population as either the S0(S) or the S0(P) galaxies.

4. THE ORIGIN AND FATE OF THE ISM IN EARLY GALAXIES

What does the striking relationship between the amount of cool interstellar matter and the morphology of the galaxy mean? The few ellipticals with neutral hydrogen might plausibly have acquired their gas in the course of a recent merger. In spirals it is believed that the gas observed now is the residual of the primordial gas, modified by the input from evolving stars and the loss of material in star forma-

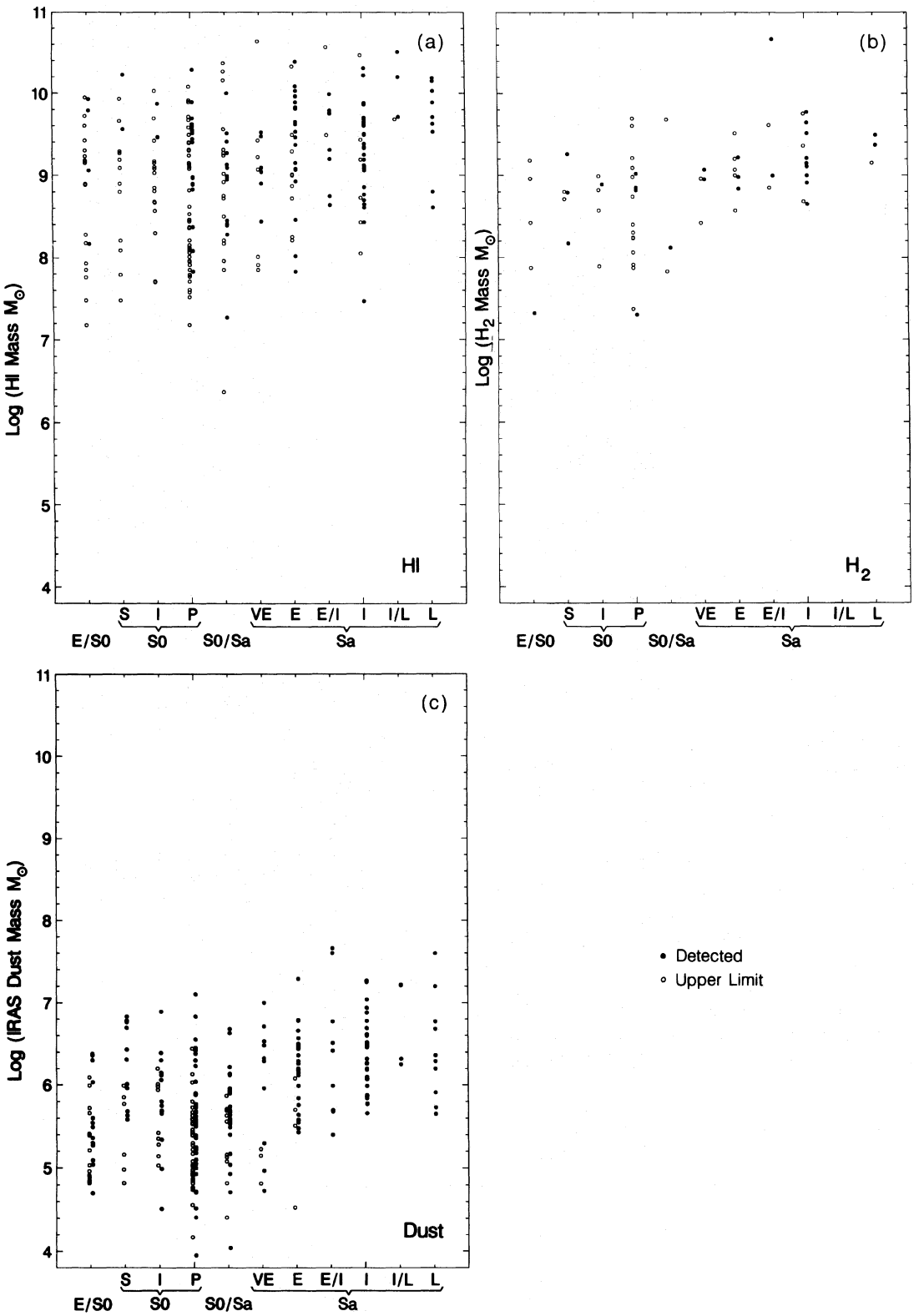

FIG. 2. The mass of cool interstellar material of various types as a function of galaxy subtype. Filled circles denote detections, open circles denote upper limits. (a): neutral hydrogen. (b): molecular hydrogen, as deduced from CO measurements. (c): dust, as deduced from *IRAS* measurements,

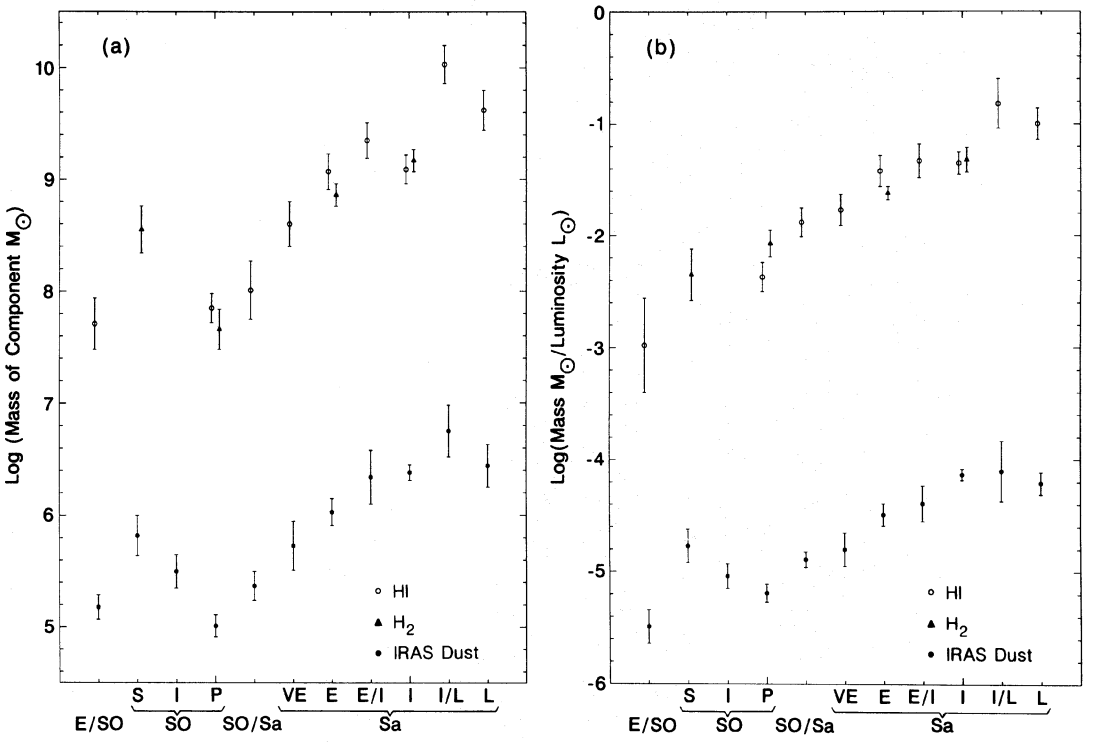

FIG. 3. The mean values of mass, and the error in the mean, for each cool matter component as a function of galaxy subtype. (a): mass values in solar units. (b): mass values normalized by blue luminosity, in solar units.

tion (Roberts 1963; Sandage 1986). Presumably the S0 and Sa galaxies represent some intermediate stage of this equilibrium. We can use the estimate of total cool matter to put constraints on the rate of star formation in these galaxies.

Figure 6 shows the average surface density of hydrogen (H I+H_2) as a function of galaxy type and subtype. The average surface density, a quantity independent of distance, has been calculated by dividing the total mass in hydrogen by the area of the galaxy, assumed to be circular of diameter set by the size of the isophote at optical brightness of 25 mag arcsec.$^{-2}$ We have distinguished the estimates of total mass that are based on direct measurements of the gas (filled circles) and those that are inferred from infrared data only (filled triangles). Upper limits are denoted by the open circles. The mean value and the error in the mean have been estimated as before, using the Kaplan–Meier (K–M) estimator, and are shown in the figure by the large circles. The average surface density increases in the later classes.

Since the fraction of objects which are detected is a strong function of galaxy morphology, and since for some subtypes the smallest value is an upper limit, rather than a detection, it is important to examine the possible uncertainties inherent in the application of the K–M estimator to confirm that the trend of surface density with morphology is not an artifact of the sampling. As has been discussed by Haynes *et al.* (1990), the mean will be biased in the case

TABLE 6. Average values of luminosity and distance for the subtypes.

Subtype	Number of Galaxies	log <L> (L in $L_\odot$)	σ	<D> Mpc	σ
E/S0	29	10.69	0.80	37.4	19.8
S0(S)	19	10.69	0.70	40.2	20.0
S0(I)	25	10.74	0.71	47.0	22.8
S0(P)	88	10.38	0.93	31.6	18.6
S0/Sa	41	10.48	0.82	35.0	17.8
Sa(VE)	17	10.73	1.03	35.1	15.4
Sa(E)	31	10.62	0.74	41.3	21.2
Sa(E/I)	10	10.84	0.73	47.5	33.6
Sa(I)	38	10.63	0.76	35.0	16.3
Sa(I/L)	4	10.88	0.46	39.4	7.2
Sa(L)	12	10.76	0.74	41.4	22.4

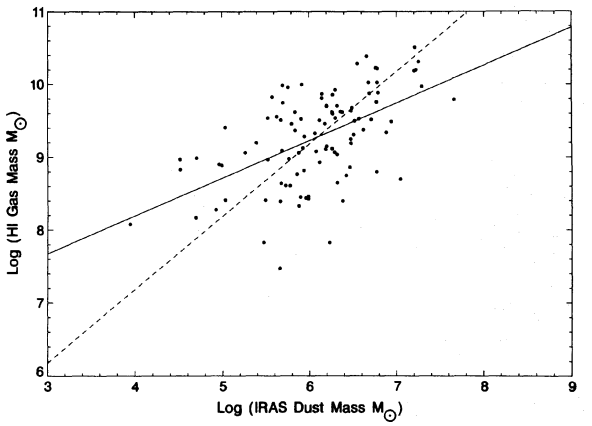

FIG. 4. The mass of neutral hydrogen as a function of the mass of dust, for objects in which both are detected. The solid line is the least-squares fit, the dashed line is the fit with a slope of 1.

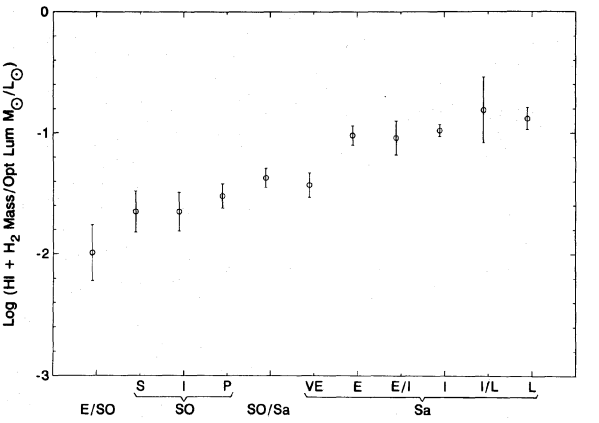

FIG. 5. The mean value of the total mass of H I and H_2, normalized by the blue luminosity, as a function of galaxy subtype. The vertical lines show the errors in the means.

where the lowest value of total mass is an upper limit. In addition, the uncertainty in the mean value is likely to be larger than expected on the basis of the variance.

We have computed three other characteristics of the sample which we used to explore the possible bias in the estimate of the mean. These are the median value of the estimator, the mean value of a data sample in which all limits less than the smallest detected mass are excluded, and an upper limit to the mean obtained by assuming that the actual masses of the objects are at the assigned limits. The mean of the truncated set must be higher than that of the entire sample, and the upper limit is an extreme value, because of the manner in which it was calculated. It is therefore satisfactory that the mean values lie typically within a factor of two of the extreme upper limit, and thus can be in error by no more than that factor. Moreover, the mean values are within a factor of 1.5 of those of the truncated set. We conclude that although there may be some bias in the mean, the magnitude cannot be great enough to have produced the trend shown in Fig. 6.

Because the estimate of surface density is heavily dependent on the *IRAS* measurements, and since the estimate of molecular mass from the flux at 100 μm is uncertain because of the uncertainties in the dust temperature and com-

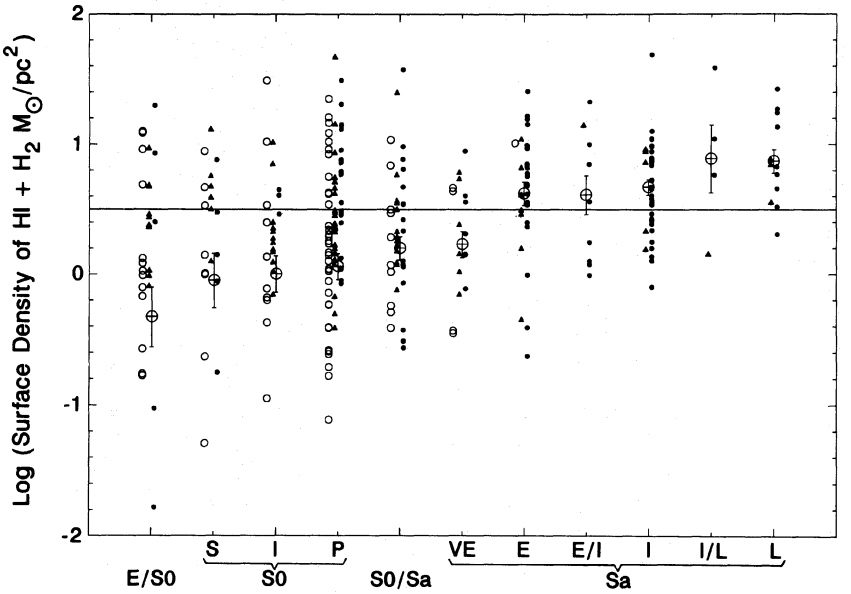

FIG. 6. The total surface density of hydrogen H I+H_2, as a function of galaxy subtype. The filled circles are objects in which hydrogen was detected, the filled triangles are objects for which the total density was inferred from infrared measurements alone, and the small open circles are upper limits. The large circles give the mean values and the errors in the means. The horizontal line indicates a value of surface density below which star formation is expected to be inhibited.

position, as was discussed in Sec. *3.3*, it is important to note that in Fig. 6 the surface densities inferred from the infrared data alone are comparable to those derived from the direct measurement of the gas. Coupled with the fact that the trends of the masses of the individual components of the cool interstellar medium are quite similar (Fig. 3), the similarity between the two groups of detected points in Fig. 6 argues that the trend of increasing surface density with later galaxy morphology arises because of an increase in the amount of material, rather than a change in some

TABLE 7. Revised values of the logarithm of the mass of cool dust.

Name	Type	60 μm		100 μm		Dust
		flux	err	flux	err	Lg Mass
		mJy		mJy		$M_\odot$
N 821	10	0	42	440	104	5.52
N 1339	10	0	27	600	51	5.30
N 1395	10	50	26	300	42	5.22
N 1399	10	0	32	270	72	5.03
N 1404	10	0	28	240	49	4.98
N 1439	10	0	32	300	35	5.23
N 1453	10	0	39	670	113	6.36
N 1537	10	0	27	260	72	4.95
N 2749	10	0	35	380	80	6.16
N 2986	10	0	25	360	109	5.53
N 3872	10	0	41	360	65	5.90
N 4168	10	0	37	590	116	5.20
N 4365	10	0	45	580	106	5.39
N 5638	10	0	30	400	116	5.20
N 5982	10	0	33	330	31	5.87
N 6876	10	90	35	430	92	6.13
N 7144	10	90	34	290	95	5.36
N 7619	10	0	38	630	205	6.36
N 2672	17	0	45	440	45	6.18
N 584	21	0	41	520	90	5.65
I 5328	21	0	31	600	54	6.12
I 4889	22	160	72	410	73	5.75
N 7192	22	0	28	270	53	5.68
N 3384	25	0	39	400	75	4.52
N 1366	30	0	28	380	54	5.09
N 1726	30	50	31	300	76	6.03
N 3610	30	0	31	250	76	5.30
N 7041	30	0	46	440	80	5.54
N 254	40	0	41	570	78	5.53
N 1440	40	0	43	1150	88	5.74
N 1543	40	0	28	1430	304	5.40
N 3637	40	0	48	1280	105	5.90
N 5422	40	70	27	330	71	5.49
N 7585	40	120	42	310	70	5.94
N 1350	50	0	190	3970	470	6.20
N 1371	50	0	135	1170	190	5.70
N 1452	50	0	135	920	110	5.84
N 2179	50	0	135	1310	200	6.29
N 3358	50	0	165	1970	235	6.50
N 3898	50	0	195	2050	250	5.84
N 4224	50	0	135	1020	120	6.18
N 4378	50	0	135	1370	160	6.27
N 4586	50	0	180	1720	200	5.68
N 4698	50	0	157	1830	210	5.70
N 4866	50	150	52	910	145	5.40
I 5240	50	0	150	1240	200	5.91
N 5701	50	0	135	1110	220	5.76
N 5864	50	0	27	340	53	5.43
N 7096	50	0	215	1130	135	6.32

physical condition such as dust temperature which affects the infrared-based mass estimate.

The important implication of Fig. 6 is that star formation is not likely to be currently active in galaxies much earlier than about Sa(I), if the criterion of Kennicutt (1989; Fig. 8) is applied, that the surface density of the star-forming material must exceed $3\mathscr{M}_\odot\,\mathrm{pc}^{-2}$. This is of course what is implicit in the assignment of the galaxy subtype, since it is not until the latest subtypes of the Sa's that the disk appears to have the lumpy structure that is a manifestation of O stars and H II regions. There are a number of objects in Fig. 6 which have surface densities greater than the criterion. Most of these are Sa's, where star formation may have started. The S0's with higher surface density perhaps have some inhibiting phenomenon (for example the absence of a spiral density wave trigger) that has slowed the formation of at least the massive stars.

Since the presence of luminous young stars is manifested by strong emission in the infrared, we have examined the infrared luminosity of our galaxy sample. As can be inferred from Fig. 2(c), the early galaxies are generally underluminous in the infrared in comparison with the later galaxies. If we take the infrared emission from a group of Sc galaxies as a point of reference, we find the difference is at least an order of magnitude for galaxies earlier than Sa, and is still a factor of about 3 even for the Sa galaxies. The difference in the ratio of infrared-to-optical fluxes between the S0 galaxies and the Sa galaxies is very marked. Using survival analysis on these data, it is found that the probability that the ratios for the S0 galaxies and the Sa galaxies are drawn from the same parent population is less than 1 percent.

Unresolved by this discussion is the question as to whether the relatively low emission in the infrared arises because of a lack of dust, or because the population of OB stars is small and unable to heat the dust effectively. We find that the infrared emission is in general greater for objects having a smaller value of the color index $(U-B)$. This suggests that the principal reason for an absence of infrared emission is a lack of radiative heating, rather than a lack of dust. Again, this is consistent with the view that the S0's and early Sa's simply do not have a population of massive young stars.

The picture that is presented by the data for early-type galaxies in the RSA2 catalog is clear: *the prominence of the disk closely mirrors the amount of cool gas which the disk contains.* Ellipticals have little dust or cool gas and no disks. The amount of interstellar hydrogen, both as H I and as H_2, smoothly increases through the S0 class to the Sa class, finally reaching an apparent saturation at a value of approximately $10^{10}\mathscr{M}_\odot$. Active star formation develops only in the later types. In the early types, the surface density of cool matter is simply too low to support general star formation. In Sa galaxies star formation is still weak, except in localized regions. Star formation does occur in certain early peculiar galaxies, but this activity appears to have been triggered by interaction with a companion galaxy. It is not until the Sb and Sc types, where there is a significant amount of cool interstellar material coupled with a triggering mechanism, that star formation occurs routinely in most objects of the class.

APPENDIX

An error has been found in the calculation of the dust masses presented in Table 2 of Paper I. The error occurs in those cases where the 60 μm flux is lacking, and we assume a dust temperature of 30 K. Equation (8) should read

$$\mathscr{M}(\mathrm{dust}) = 0.576F(100)\times D^2. \qquad \text{(A1)}$$

The values for galaxies detected at 60 μm are correct. All upper limits are in error, by 0.65 in the logarithm of the mass, in the sense that the correct upper limit is smaller than that given in Table 2 of Paper I. There are also 49 galaxies with masses listed in the table that are incorrect, because the 60 μm flux is absent although they were detected at 100 μm. Table 7 lists the correct values of the dust mass for these objects. Again, the logarithm of the correct mass is approximately 0.65 smaller than the corresponding value given in Paper I.

REFERENCES

Bregman, J. N., Hogg, D. E., & Roberts, M. S. 1992, ApJ, 387, 484 (Paper II)

de Vaucouleurs, G., de Vaucouleurs, A., & Corwin, H. G. 1976, Second Reference Catalogue of Bright Galaxies (University of Texas, Austin) (RC2)

de Vaucouleurs, G., de Vaucouleurs, A., Corwin, H. G., Buta, R. J., Paturel, G., & Fouque, P. 1991, Third Reference Catalogue of Bright Galaxies (Springer, New York) (RC3)

Eder, J., Giovanelli, R., & Haynes, M. P. 1991, AJ, 102, 572

Eskridge, P. B., & Pogge, R. W. 1991, AJ, 101, 2056

Feigelson, E. D., & Nelson, P. I. 1985, ApJ, 293, 192

Haynes, M. P., Giovanelli, R., & Chincarini, G. L. 1984, ARA&A, 22, 445

Haynes, M. P., Herter, T., Barton, A. S., & Benensohn, J. S. 1990, AJ, 99, 1740

Isobe, T., Feigelson, E. D., & Nelson, P. I. 1986, ApJ, 306, 490

Kennicutt, R. C. 1981, AJ, 86, 1847

Kennicutt, R. C., & Edgar, B. K. 1986, ApJ, 300, 132

Kennicutt, R. C. 1989, ApJ, 344, 685

Knapp, G. R., Helou, G., & Stark, A. A. 1987, AJ, 94, 54

Knapp, G. R., Guhathakurta, P., Kim, D.-W., & Jura, M. 1989, ApJS, 70, 329

Lauberts, A. 1982, The ESO/Uppsala Survey of the ESO(B) Atlas (European Southern Observatory, Garching)

LaValley, M., Isobe, T., & Feigelson, E. 1992, in Astronomical Data Analysis Software and Systems, edited by D. Worral *et al.* (ASP, San Francisco), p. 245

Maloney, P., & Black, J. H. 1988, ApJ, 325, 389

Nilson, P. 1973, Uppsala General Catalog of Galaxies, Acta Univ. Ups., Ser. V, A, Vol. 1 (Uppsala)

Reynolds, J. H. 1927a, Observatory, 50, 185

Reynolds, J. H. 1927b, Observatory, 50, 308

Roberts, M. S. 1963, ARA&A, 1, 149

Roberts, M. S. 1975, in Galaxies and the Universe, edited by A. Sandage, M. Sandage, and J. Kristian (University of Chicago Press, Chicago), p. 309

Roberts, M. S., Hogg, D. E., Bregman, J. N., Forman, W. R., & Jones, C. 1991, ApJS, 75, 751 (Paper I)
Sandage, A. 1961, The Hubble Atlas of Galaxies (Carnegie Institute of Washington, Washington)
Sandage, A. 1983, in IAU Symposium 100, edited E. Athanassoula (Reidel, Dordrecht), p. 367
Sandage, A. 1986, A&A, 161, 89
Sandage, A., & Bedke, J. 1993, Carnegie Atlas of Galaxies (Carnegie Institute of Washington, Washington, DC)
Sandage, A., Freeman, K. C., & Stokes, N. R. 1970, ApJ, 160, 831
Sandage, A., & Tammann, G. A. 1981, A Revised Shapley–Ames Catalog of Bright Galaxies (Carnegie Institution of Washington, Washington) (RSA1)
Sandage, A., & Tammann, G. A. 1987, A Revised Shapley–Ames Catalog of Bright Galaxies (Carnegie Institute of Washington, Washington) (RSA2)
Thronson, H. A., Tacconi, L., Kenney, J., Greenhouse, M. A., Margulis, M., Tacconi-Garman, L., & Young, J. S. 1989, ApJ, 344, 747
Young, J. S., & Scoville, N. Z. 1991, AR&A, 29, 581
Young, J. S., Shuding Xie, Kenney, J. D. P., & Rice, W. L. 1989, ApJS, 70, 699